SCHARGEV 1.0 - SSC Vlasov solver SINGLE BUNCH

Tim Zolkin, Alexey Burov

Fermi National Accelerator Laboratory

zolkin@fnal.gov, *burov@fnal.gov*

June 28, 2016

TABLE OF CONTENTS

Abstract

The space charge (SC) is known to be one of the major limitations for the collective transverse beam stability. When SC is strong (i.e. space charge tune shift $\gg$ synchrotron tune) the problem allows an exact analytical solution. For that practically important case we present a fast and effective Vlasov solver SCHARGEV which calculates a complete eigensystem (spatial shapes of modes and bunch spectra) and therefore provides the growth rates and the thresholds of instabilities. SCHARGEV allows an inclusion of driving and detuning wake forces, coupled bunch motion, any feedback system and Landau damping. In this presentation we will consider a Gaussian bunch under the action of resistive wall wakes and damper. A numerical example for FermiLab Recycler Ring is given.

1. Introduction. What do we know about SSC?

PHYSICAL REVIEW SPECIAL TOPICS - ACCELERATORS AND BEAMS **12**, 044202 (2009)

Head-tail modes for strong space charge

A. Burov

PHYSICAL REVIEW SPECIAL TOPICS - ACCELERATORS AND BEAMS **12**, 124402 (2009)

Transverse modes of a bunched beam with space charge dominated impedance

V. Balbekov*

PHYSICAL REVIEW SPECIAL TOPICS - ACCELERATORS AND BEAMS **17**, 021007 (2014)

Nested head-tail Vlasov solver

A. Burov

Coupled-Beam and Coupled-Bunch Instabilities

A. Burov*
Fermilab, PO Box 500, Batavia, IL 60510-5011

Rigid-slice approximation

When the space charge tune shift in the 3D center of a bunch is much larger than both the synchrotron tune Q_s and the wake-driven coherent tune shift Q_W

$$Q_{max} \gg Q_s, Q_W$$

the separation between the coherent frequency and the incoherent spectrum is larger than the width of the bare incoherent spectrum, and, the *rigid-slice approximation* can be used.

Burov Equation

SSC rigid beam (no-wake eigensystem)

$$\boxed{\frac{\mathrm{d}}{\mathrm{d}\tau}\left(u^2(\tau)\frac{\mathrm{d}\,Y(\tau)}{\mathrm{d}\tau}\right)+\nu\,Q\,Y(\tau)=0}$$

$Q_W \gg Q_s^2/Q_{\max}$ and damper: $\mathcal{Y}_k(\tau)=\sum_{i=0}^{\infty}\mathbf{C}_i^{(k)}\,Y_i(\tau)$

$$\frac{\mathcal{Y}''(\tau)}{\mathcal{R}(\tau)}+\omega\,\mathcal{Y}(\tau)=\left[\varkappa\left(\widehat{\mathrm{W}}+\widehat{\mathrm{D}}\right)-i\,g\,e^{i\,\psi}\,\widehat{\mathrm{G}}\right]\mathcal{Y}(\tau).$$

$$\varkappa=N_{\mathrm{b}}\,\frac{r_0\,R_0}{4\,\pi\,\gamma\,\beta^2\,Q_\beta}\,\frac{Q_{\mathrm{eff}}(0)}{Q_s^2}$$

PART II.

SCHARGEV 1.0

2 What is SCHARGEV 1.0?

$$\mathbf{M} \cdot \mathbf{C}^{(k)} = \omega_k \mathbf{C}^{(k)}$$

$$\mathbf{M} = \boxed{(\nu_l - i\,\lambda_l)\delta_{lm} + \varkappa \left[\widehat{\mathrm{W}}_{lm}(\zeta) + \widehat{\mathrm{D}}_{lm}\right] - i\,g\,e^{i\,\psi}\widehat{\mathrm{G}}_{lm}(\zeta)}$$

$$\begin{aligned}
\widehat{\mathrm{W}}_{lm} &= \int_{-\infty}^{\infty}\int_{-\tau}^{\infty} \mathrm{d}\,\sigma\,\mathrm{d}\,\tau\, W(\tau-\sigma)\,\rho(\tau)\,\rho(\sigma)\,Y_l(\tau)\,Y_m(\sigma)\,e^{i\,\zeta(\tau-\sigma)}, \\
\widehat{\mathrm{D}}_{lm} &= \int_{-\infty}^{\infty}\int_{-\tau}^{\infty} \mathrm{d}\,\sigma\,\mathrm{d}\,\tau, D(\tau-\sigma)\,\rho(\tau)\,\rho(\sigma)\,Y_l(\tau)\,Y_m(\tau), \\
\widehat{\mathrm{G}}_{lm} &= \mathrm{K}_l(\zeta)\,\mathrm{P}^*_m(\zeta),
\end{aligned}$$

where

$$(\mathrm{P},\mathrm{K})_k(\zeta) = \int_{-\infty}^{\infty} \mathrm{d}\,\tau\,(P,K)(\tau)\,\rho(\tau)\,Y_k(\tau)\,e^{i\,\zeta\,\tau}.$$

2.1 SSC harmonics for Gaussian beam

The use of longitudinal distribution function for Gaussian bunch

$$f(v,\tau) = \frac{N_\mathrm{b}}{2\,\pi\,\sigma\,u(\tau)}\,e^{-v^2/2\,u^2-\tau^2/2\,\sigma^2}$$

gives the equation for SSC harmonics

$$\boxed{y''(\tau) + \nu\,e^{-\tau^2/2}y(\tau) = 0, \qquad y'(\pm\infty) = 0},$$

where **natural system of units** is employed: the distance τ is measured in units of the RMS bunch length σ, and, ν in units of

$$\frac{u^2}{\sigma^2\,Q_\mathrm{eff}(0)} = \frac{Q_\mathrm{s}^2}{Q_\mathrm{eff}(0)}.$$

Orthonormal basis in Hilbert space

- Scan and order $\nu_0 < \nu_1 < \ldots < \nu_k < \ldots \to \infty$

- Normalize with $\int_{\infty}^{-\infty} \rho(\tau)\, y_i(\tau) y_j(\tau) \mathrm{d}\,\tau = \delta_{ij}$ where $\rho(\tau) = \frac{e^{-\tau^2/2}}{\sqrt{2\pi}}$ is the normalized line density of a beam.

SSC harmonics and chromaticity

2.2 Dipole moments and flat bunch-by-bunch damper

$$I_k(\zeta) = \int_{-\infty}^{\infty} \rho(\tau)\, Y_k(\tau)\, e^{i\,\zeta\,\tau}\, \mathrm{d}\,\tau = I_k^{\cos}(\zeta) + i\, I_k^{\sin}(\zeta)$$

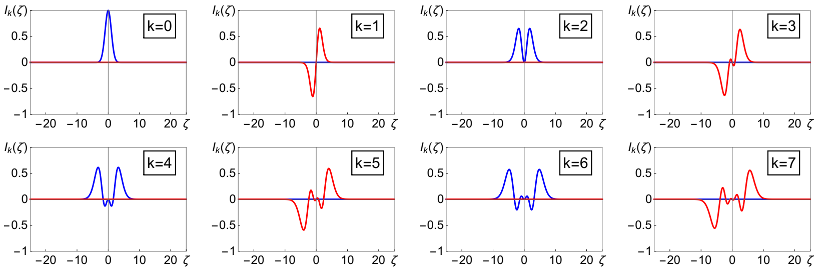

Figure: Real (blue) and imaginary (red) parts of first 8 dipole moments for the Gaussian bunch SSC harmonics as functions of chromaticity.

Abs(I_k) has max at $\zeta \approx k$

Damper matrix

$$\widehat{\mathrm{G}}_{lm} = \int_{-\infty}^{\infty}\int_{-\infty}^{\infty} \mathrm{d}\,\tau\,\mathrm{d}\,\sigma\,\rho(\tau)\rho(\sigma)\,Y_l(\tau)\,Y_m(\sigma)\,e^{i\,\zeta(\tau-\sigma)} = \boxed{I_l(\zeta)I_m^*(\zeta)}$$

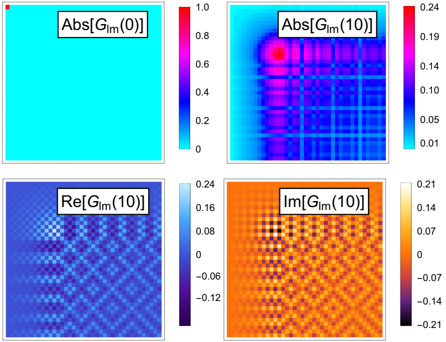

Figure: Matrices of direct product of dipole moments for $\zeta = 0, 10$.

2.3 Wake forces

Resistive wall impedance over distance L

$$W_m(\tau < 0) = J_{\mathrm{vc}} \, \frac{2}{\pi} \, \frac{1}{b^{2m+1}(1+\delta_{m0})} \sqrt{\frac{c}{\sigma_{\mathrm{s}}}} \, \frac{L}{\sqrt{|\tau|}},$$

b — vacuum chamber radius
J_{vc} — Yokoya factor
σ_{s} — conductivity

$$\varkappa \to \kappa = N_{\mathrm{b}} \, \frac{r_0 R_0}{4\,\pi\,\gamma\,\beta^2\,Q_\beta} \, \frac{Q_{\mathrm{eff}}(0)}{Q_{\mathrm{s}}^2} \, \frac{2\,L\,\sqrt{c/\sigma_{\mathrm{s}}}}{\pi\,b^3},$$

$$W(\tau) = \frac{\mathrm{H}(\tau)}{\sqrt{|\tau|}} \qquad \text{and} \qquad \overline{W}(\omega) = \sqrt{\frac{\pi}{2}}\,\frac{1 + i\,\mathrm{sgn}(\omega)}{\sqrt{|\omega|}}.$$

Driving wake

$$\boxed{\widehat{\mathrm{W}}_{lm}(\zeta) = \int_{-\infty}^{\infty} \overline{W}(\omega - \zeta) I_l(\omega) I_m^*(\omega) \frac{\mathrm{d}\,\omega}{2\pi}}$$

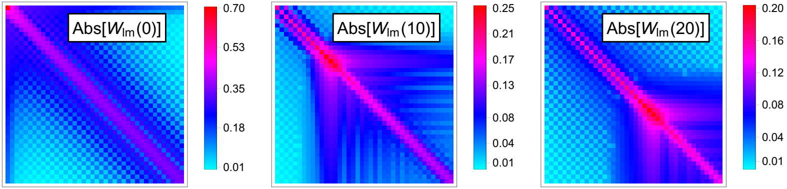

Figure: Absolute values of driving resistive wall wake matrices $\widehat{\mathrm{W}}_{lm}(\zeta)$.

Detuning wake

$$\boxed{\widehat{\mathrm{D}}_{lm} = \int_{-\infty}^{\infty} D(\tau)\rho(\tau)Y_l(\tau)Y_m(\tau)\,\mathrm{d}\tau}, \qquad D(\tau) = \int_0^{\infty} \frac{\rho(\sigma+\tau)}{\sqrt{\sigma}}\,\mathrm{d}\sigma.$$

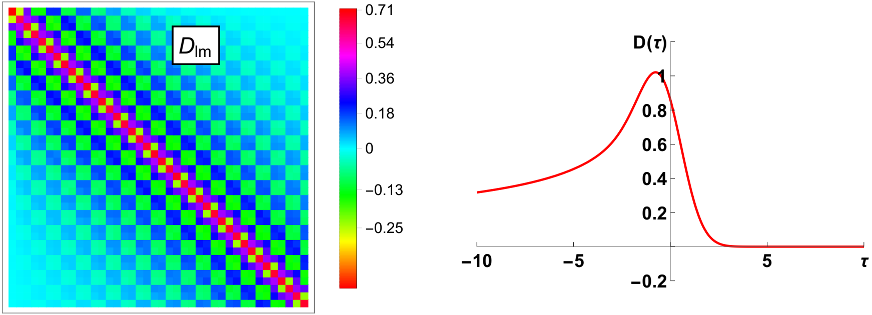

Figure: Detuning wake matrix $\widehat{\mathrm{D}}_{lm}$ and quadrupole wake field.

PART III.
RESULTS AND DISCUSSION

3.1 DAMPER

Damper eigenproblem

$$\Big[\mathrm{diag}(\nu_k) - i\, g\, e^{-i\,\psi}\, \widehat{\mathrm{G}}(\zeta)\Big]\, \mathbf{C} = \omega\, \mathbf{C}.$$

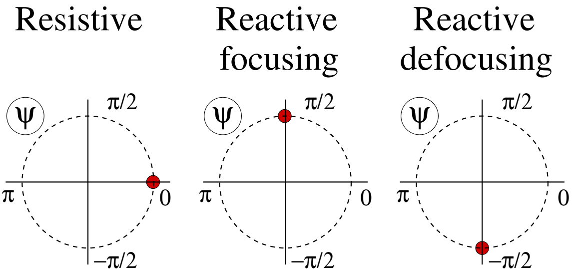

Resistive damper, $\psi = 0$

For $|2\zeta| < |g|$ damper forms a rigid bunch mode.

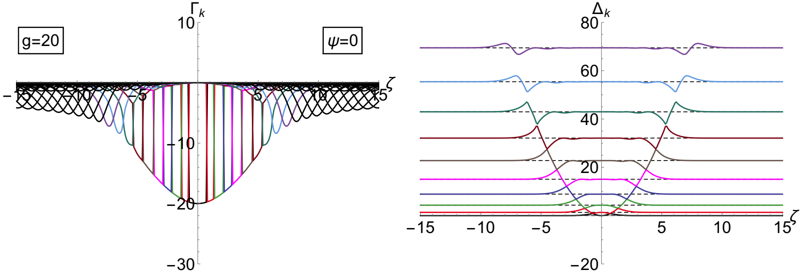

Figure: Bunch spectrum for resistive damper as a function of ζ. Modes are ordered with respect to $\Re\omega_k$ (all modes with $k > 10$ are shown in black). Dashed lines show unperturbed frequencies $\Delta_k = \nu_k$.

Reactive damper, $\psi = \pm\pi/2$

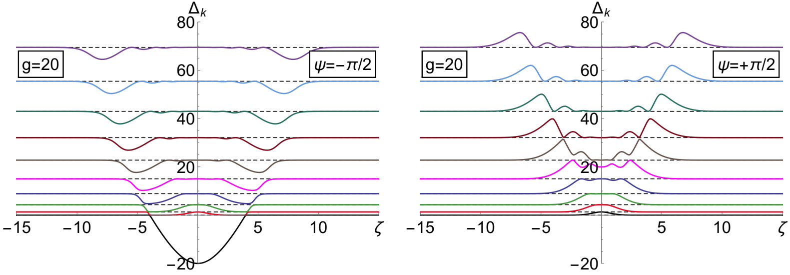

Figure: Real part of bunch spectrum for defocusing (left) and focusing (right) reactive dampers. Modes are ordered with respect to $\Re\omega_k$. Dashed lines show unperturbed frequencies $\Delta_k = \nu_k$.

Damper asymptotic, $|g| \gg |2\zeta|$

Damper sight band is determined by $\Delta_k \approx \zeta^2$

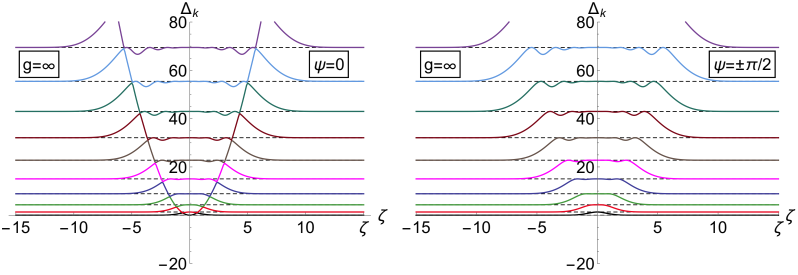

Figure: Real part of bunch spectrum for infinitely powerful resistive (left) and reactive (right) dampers. Modes are ordered with respect to $\Re\,\omega_k$. Dashed lines show unperturbed frequencies $\Delta_k = \nu_k$.

Damper and modes

3.2 TMCI at $\zeta = 0$.

Wake eigenproblem

$$\mathrm{R} \quad : \quad \omega\,\mathbf{C} = \left[\mathrm{diag}\,\nu_k - \kappa\,\widehat{\mathrm{W}}_{lm}(\zeta)\right]\mathbf{C},$$

$$\mathrm{V} \quad : \quad \omega\,\mathbf{C} = \left[\mathrm{diag}\,\nu_k - \kappa\,\widehat{\mathrm{W}}_{lm}(\zeta) - \frac{\kappa}{2}\,\widehat{\mathrm{D}}_{lm}\right]\mathbf{C},$$

$$\mathrm{H} \quad : \quad \omega\,\mathbf{C} = \left[\mathrm{diag}\,\nu_k - \frac{\kappa}{2}\,\widehat{\mathrm{W}}_{lm}(\zeta) + \frac{\kappa}{2}\,\widehat{\mathrm{D}}_{lm}\right]\mathbf{C}.$$

Convergence with number of modes

Round chamber (R) and flat chamber vertical dof (V)

All coherent tune shifts are < 0 and TMCI caused by coupling of 0-th and 1-st modes.

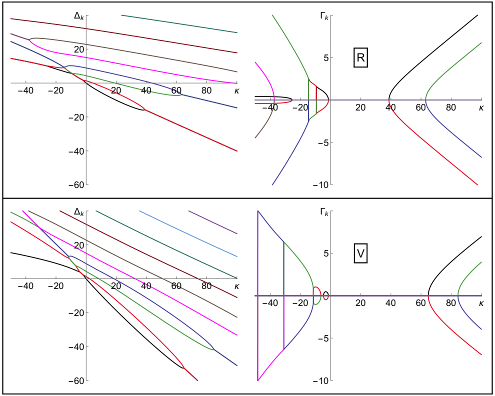

Flat chamber horizontal dof (H)

All coherent tune shifts are > 0 and TMCI caused by coupling of 6-th and 7-th modes.

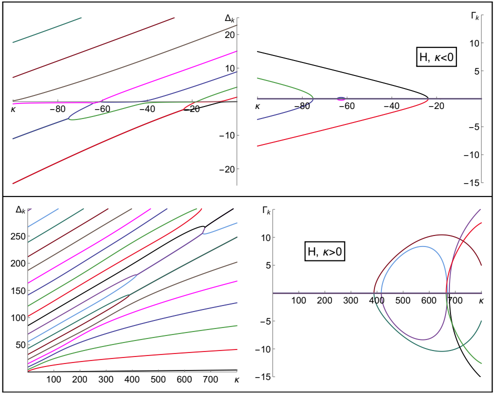

Resistive and reactive damper vs. TMCI at $\zeta = 0$

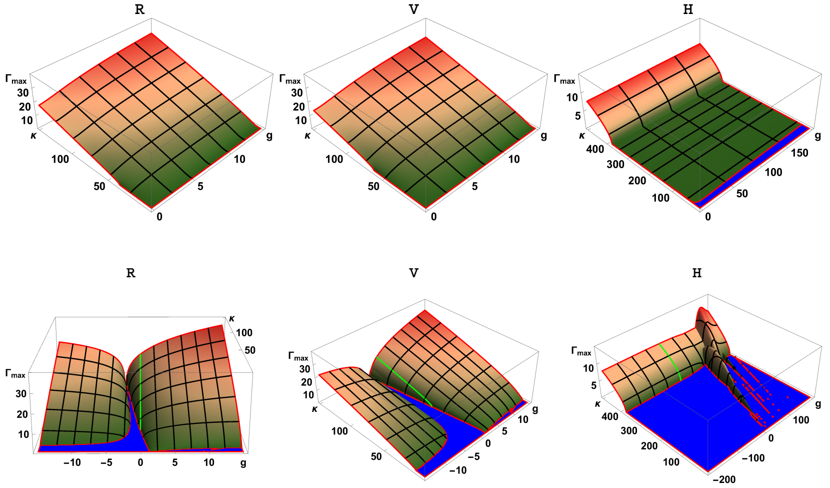

3.3 Instability for $\zeta \neq 0$

Without damper when $\zeta \neq 0$ beam is unstable $\forall\, \kappa$!

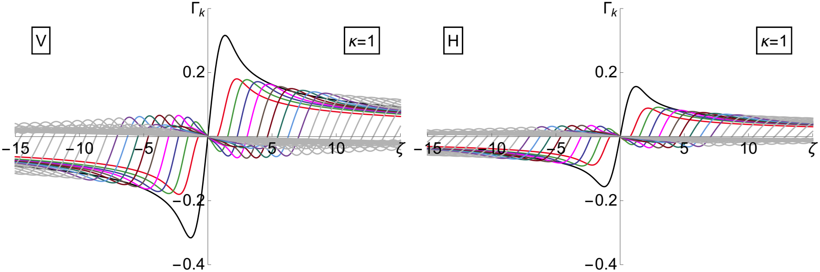

It looks like one need to operate an accelerator at $\zeta < 0$ below the transition energy (and $\zeta > 0$ above the transition)

Resistive damper will help now

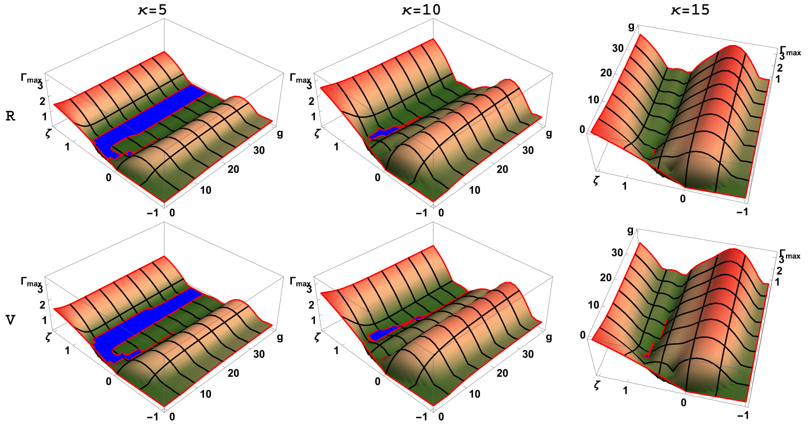

Note that the chromaticity sign is opposite to conventional!!!

Horizontal degree of freedom can be stabilized as well

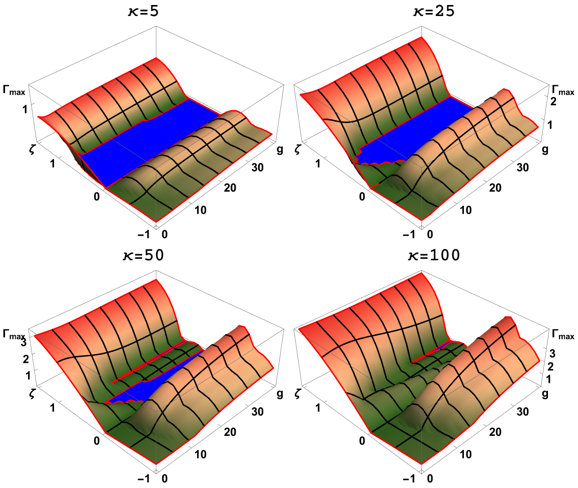

4. Summary

• The fast and efficient Vlasov solver SCHARGEV 1.0 has been created. It includes driving and detuning resistive wall wakes and feedback. (*work on Landau damping and couple-bunch wakes in progress*)

• Thresholds and nature of TMCI for SSC Gaussian beam

	Damper phase	R	V	H
$\zeta = 0$	—	40	65	390
	$-\pi/2$	$\approx$ 100	$\approx$ 150	390
$\zeta \neq 0$	0	$\approx$12	$\approx$14	$\approx$100

• For $\zeta = 0$ defocusing reactive damper can be used to increase the TMCI threshold ($\approx$ 2–3 times) for round and vertical dof of flat chambers.

• For $\zeta \neq 0$ the resistive damper will stabilize the instability for $|\zeta| < 1$.

Note that the chromaticity sign is opposite to conventional.

• "Lake of stability" with $\zeta \neq 0$ should be used due to its structural stability and since its measure $2 > 1$ — measure of "river" at $\zeta = 0$.

LAST SLIDE

Thank you for your attention!

Questions?